

INVESTIGATIONS INTO SEISMIC FAILURE OF HIGH ARCH DAM BASED ON SHAKING TABLE EXPERIMENTS AND NUMERICAL SIMULATION

Fan Shuli¹, Chen Jianyun², and Wang Jianyong³

¹ Lecturer, State Key Laboratory of Coastal and Offshore Engineering, Dalian University of Technology, Dalian, China

² Professor, State Key Laboratory of Coastal and Offshore Engineering, Dalian University of Technology, Dalian, China

³ Assistant engineer, Jiangsu Transportation Research Institute, Nanjing, China
Email: shuli@dlut.edu.cn, eerd001@dlut.edu.cn, motorlia@163.com

ABSTRACT :

A series of shaking table tests was performed on several small-scaled models of an arch dam of 210 m in height using a suitable model material. The purpose of the tests was to assess the possible failure mechanisms of medium to high arch dams and its behaviors under strong earthquakes. The studies on the shape, position, occurrence conditions and influence factors of dynamic cracks in dam body have been conducted in combination with shaking model test and numerical analysis using an elastic damage constitutive model. The results of the numerical simulations indicate final failures of model dam calculated using the double lines damage model of residual strength are in agreement with the test results. The cracks normally appeared near the top of arch crown and one-quarter points of both sides

KEYWORDS: arch dam, shaking table, cracking, damage, seismic properties

1. INTRODUCTION

Nearly 70% of national total hydropower potential is concentrated in the southwest of China, the region is well known for its high seismic intensity and frequent occurrence. About 40% of dams, with a reservoir more than 100 million cubic meters in volume, are located in the area of seismic intensity larger than VII, and 13% in the area of seismic intensity larger than VIII. Consequently, seismic safety of large dams presents a difficult problem in the design. Real behavior of structures under strong earthquake is very important for an aseismic design, especially the cracking of concrete, which produce failure of the dam, having catastrophic consequences on the downstream life and property. In order to prevent serious damage of dam at rare seismic attack, it is important to find out the place of structural weakness, the development of damage on the dam system as well as the ultimate aseismic capacity of the dam. Moreover, there is still insufficient experience and appreciation of the dynamic behavior and seismic failure mechanisms of high arch dams during strong earthquakes [Zhou and Lin 2000]. Currently, design codes treat an arch dam as a linear monoblock, even though investigations have indicated that arch dams exhibit nonlinear response to strong earthquakes.

Non-linear seismic response evaluation of concrete dams has received considerable attention during the last couple of decades. The prediction of seismic responses of dams depends mainly on mathematical model [Fenves and Mojtahedi 1992]. It is unavoidable that simplification in mathematical model and approximation in many parameters have to be made in numerical analysis and designs, mostly based on experience of engineers. The absence of experience and field data makes it difficult to verify these numerical results, which motivates laboratory experiments on a scaled model.

Dynamic rupture model test is one of method to research the nonlinear dynamic response and damage pattern of structures, and to verify the numerical analysis method. With the development and requirement of engineering practice and numerical technology, the model test with structure nonlinear rupture considered is more and more important. A few shaking table tests of arch dam were performed by Chen and Li [1995, 1996], by Wang and Li [2006, 2007], and by Zhou et al. [2000]. In this paper, a series of shaking table tests was performed on several small-scaled models of an arch dam using a suitable model material. The purpose of the tests was to

assess the possible failure mechanisms of medium to high arch dams and its behaviors under strong earthquakes. The studies on the shape, position, occurrence conditions and influence factors of dynamic cracks in dam body have been conducted in combination with shaking model test and numerical analysis using an elastic damage constitutive model.

2. MODEL MATERIAL

The characteristics of the model material are very important for dynamic failure experiments, especially for small-scales dynamic model test. For dynamic failure experiments, the gravity similarity must be satisfied, and the model material should have low intensity and high density, and the stress and strain relations of the model material and prototype concrete should be similar after yielding. These requirements made the development of a suitable model material into a long and costly process. Considerable work has been done in previous studies to produce an appropriate similitude model material [Lin and Zhou 1993, Zhou and Lin 2000, Fan and Chen 2007]. This special material consists of cement, river sand, heavy quartz sand, heavy quartz powder, iron powder, and water, in the ratios by mass of 1.0, 5.09, 29.41, 9.0, 0.05 and 3.85 respectively. Its density and Poisson's ratio approach those of prototype concrete. The normalized stress and strain curves of similitude model material and prototype concrete are shown in figure 1. The Typical compressive and tensile fracture modes are shown in figure 2. These show that the characteristics of the model material agree well with those of mass concrete. Its tensile strength and modulus of elasticity are much lower than these of mass concrete and are controlled by its age. Normally, it takes 8 h to mold a dam model and another 72 h to cure it in a suitable laboratory environment, which consists of a temperature range of 15-18c and a humidity range of 50-70%. The strengths of the model material for seismic failure experiments were 0.30-0.70MPa in compression and 0.03-0.09MPa in tension. The dynamic young's modulus of elasticity and density were, respectively, in the ranges of 600-1000MPa and 2400-2700 kg/m³. Measured damping ratio of the model material was 2.1% with attenuation method.

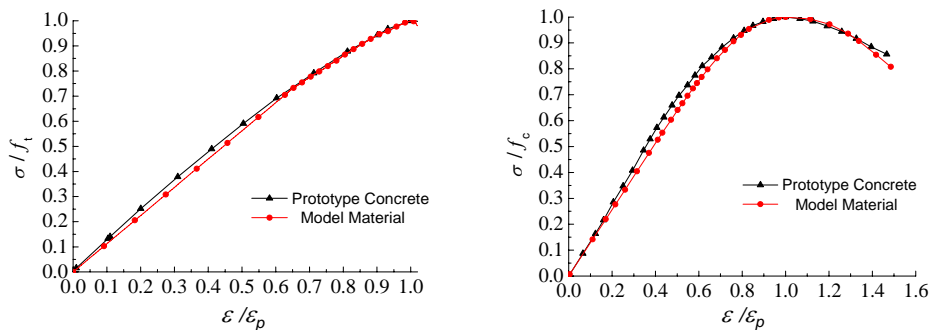


Figure 1 Normalized stress-strain curves of model material and prototype concrete

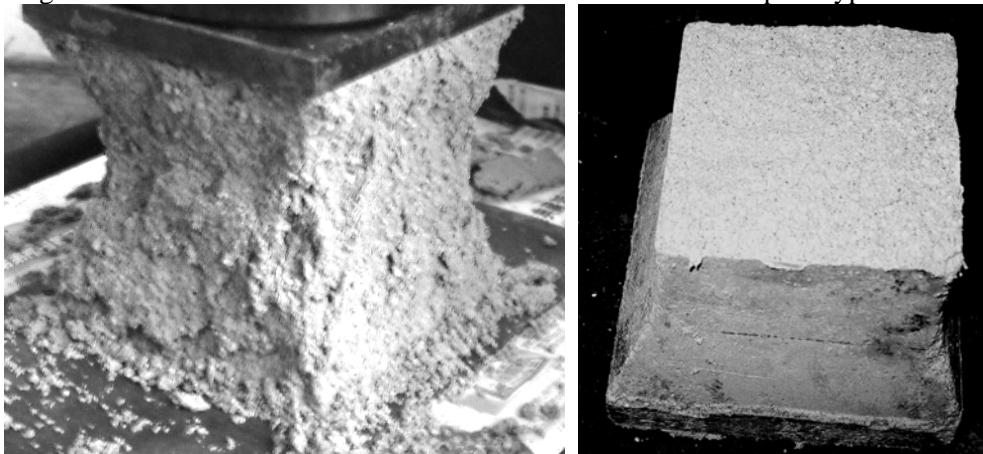


Figure 2 Typical compressive and tensile fracture modes of model material

3. EXPERIMENTAL PROGRAM

3.1. Brief Introduction of to the Project

The Dagangshan arch dam under study is to be built on Dadu River. The tallest crown of the dam is 210 m in height, 10 m in thickness at the crest and 55 m at the base, and the crest length is 609.8 m. The dam site is situated on an earthquake active zone of china with high seismicity. According to results of the investigation on local geology and seismic environment and seismic risk analysis, the intensity at the dam site is VIII and the peak ground acceleration (PGA) for design is 0.557 g with a 0.2% probability of this being exceeded in 100 years accordingly.

3.2 Description of Dam Model

The model system included the arch dam, partial foundation rock with topographic feature near the dam. The ratio scale in geometry was taken as 1/273 so that the model dam was 2.0 m in width and 0.77 m in height. The height of the foundation was 0.2 m, horizontal extensions were 0.35 and 0.45 m in both upstream and downstream direction at dam abutment, respectively. Total weight of the test model was about 9,000 kg and the volume was about 3.16 m³. The completed model is shown in figure 3. Major ratio scales of the test are listed in Table 3.1.



Figure 3 Test models

Table 3.1 Ratio of scale of test model

Physical dimension	Scale ratio
Geometry	273
Density	1.0
Elastic modulus	273
Acceleration	1
Time	16.5
Frequency	0.06
Stress	273
Strain	1

3.3. Test Instrumentation

Three types of data have been measured, response accelerations on the dam as well as those along the valley, dynamic strains and displacements of the dam. Nine AR-5F acceleration transducers were used. The accelerometers measured the horizontal crest accelerations and the table base accelerations. Two BJQN-4B bridge deflection detectors have been used to measure displacements in radial direction on the crest relative to the dam foundation. Fourteen Fiber Bragg Grating (FBG) strain sensors (shown in figure 4) were used to measure the dam deformation. The sensors positions were plotted in figure 5.



Figure 4 FBG strain sensor

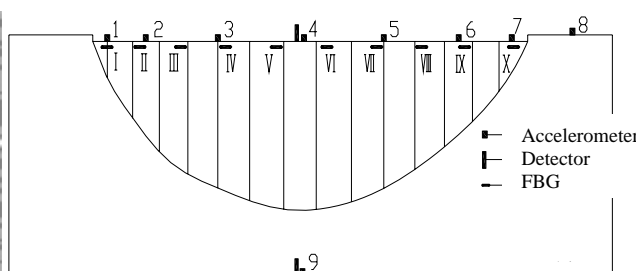


Figure 5 Layout of sensors

4. TEST RESULTS

4.1. Test program

In this series of model tests, two sets of different waves were used. Seismic motion was applied on the dam system in horizontal and vertical directions simultaneously, where the level in vertical direction was 2/3 of that in horizontal. Twelve dam models, of three different types (monoblock model, model with two contraction joints, and model with three contraction joints), were tested using artificial waves or cite waves. Totally 15 different cases of test have been carried out, including different level of waves, as summarized in table 4.1. In this paper, the monoblock model test results were analyzed.

Table 4.1 Dynamic loading cases

Case	1	2	3	4	5	6	7
Load level	0.05	0.10	0.15	0.20	0.25	0.30	0.35
Case	8	9	10	11	12	13	14
Load level	0.40	0.45	0.50	0.55	0.60	0.65	0.70

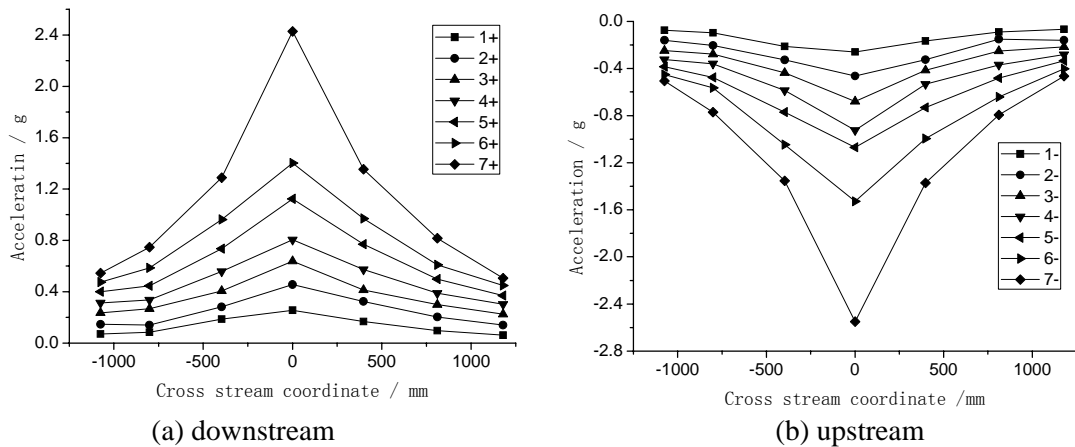
4.2. Test Results of Monoblock Model

4.2.1. Seismic response

Distributions of peak acceleration near the dam crest are shown in figures 6 in downstream and upstream direction under different level artificial waves, respectively. It is evident that the maximum acceleration is present to the top of the arch crown, and the peak accelerations decrease in turn along the canyon. Distribution of peak accelerations in stream direction on crest is nearly symmetric when excited by artificial waves. This shows that the symmetric vibration mode plays a leading role under artificial wave excitation in the stream and vertical direction. The peak accelerations exhibit a near linear increase with the increasing of earthquake level before the sixth test stage. It is clear that the increasing extent of peak acceleration increases suddenly from sixth to seventh test stage, almost reaches 73.1% (from 1.402 g to 2.427g). The dam responses were non-linear between cases 5 and 7.

The distributions of amplifications and maximum displacement on the crest are displayed in figure 7 and 8. Amplification from dam heel to crest is 9.06 times in case 10. Stream displacement at the centre of the crest is 5.48 mm in case 5, but reaches 8.22 in case 6. Combining with the measured displacement and strain (Figure 8 and 9), it is found that there had been some damage on dam face. In case 10, the displacement reaches 19.70 mm, the dam had been in failure stage. The failure caused the amplification drop from 9.06 to 5.52.

Responses of strain near the dam crest are shown in figures 9. The distributions of peak tensile and compressive strain are symmetric as same as that of peak acceleration. The dynamic strains were larger near arch crown than these near dam abutments. So the upper zone of the arch dam is the weak links.



(a) downstream (b) upstream
 Figure 6 Peak acceleration distributions in stream direction

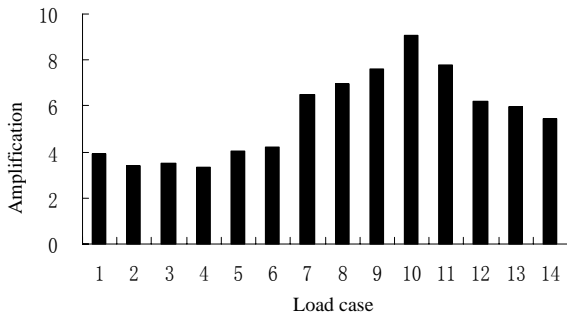


Figure 7 Amplifications in different test stage

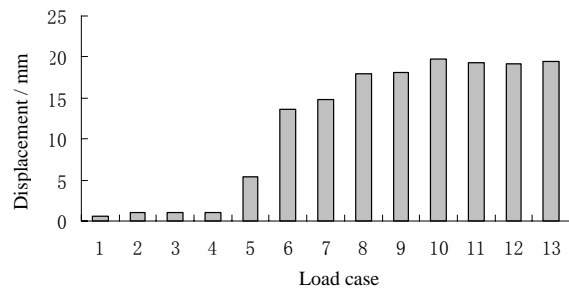
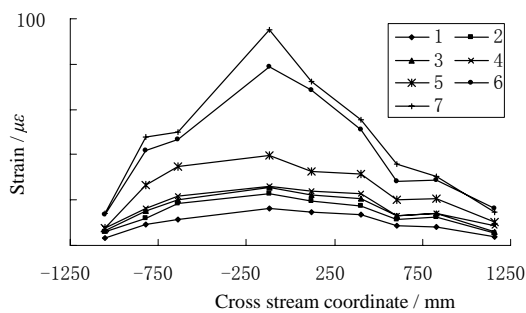
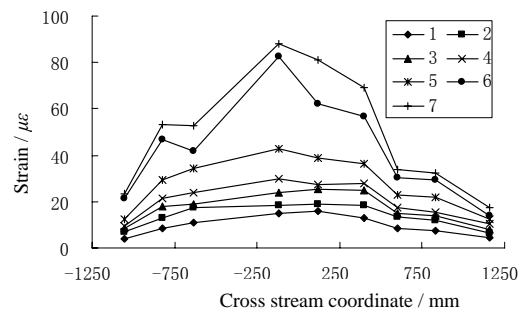


Figure 8 Relative displacement distribution



(a) tensile strain



(b) compressive strain

Figure 9 The distribution of tensile and compressive strain

4.2.3. Damage and Crack Analysis

From measured data, the opening of contact joints can be identified easily for overload cases; however, evident large opening occurs only once, as shown in Figure 17, where the minus values represent joint opening.

Damage was judged through the strain, acceleration and displacement signals changes. The damages are plotted in figure 9. It is found that there had been some damage in cantilever direction in case 10 and four cracks were appeared on the downstream and upstream face. As the increasing of load level, the number 1 crack (in figure 9) extended in 55° direction, and the height is 26 cm in case 13. The number 2 crack appeared near the arch crown and extended in vertical direction, and the height is 11 cm in case 14. Except the main cracks, some minor horizontal cracks appeared on the upstream face.

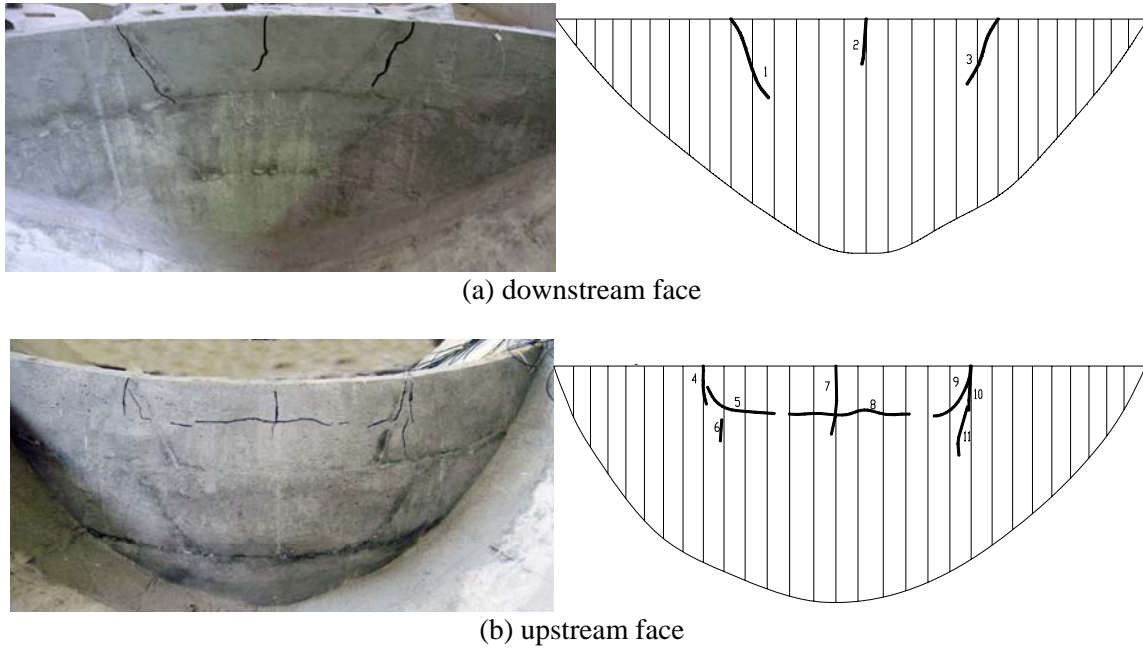


Figure 9 The failure model of dam

5. NUMERICAL SIMULATIONS

5.1. Constitutive Model

Concrete is a typical heterogeneous quasi-brittle material used in engineering, and its nonlinear characteristics in the fracture process are caused by internal crack germinating and developing. For the microscopic element, the degradation of concrete can be reflected by simple damage constitutive model. Elastic damage constitutive model was used to represent crack initiation and propagation. According to the strain equivalence principle, the constitutive relationship of damage concrete can be expressed by the nominal stress and strain, as follows

$$\sigma = E\varepsilon = E_0(1 - D)\varepsilon \quad (5.1)$$

Here, E_0 and E are undamaged elastic modulus and softened secant modulus of material. The damage parameter D varies between 0 and 1, such that $D=0$ for a virgin material, and $D=1$ for a fully cracked state. When the maximum element stress reaches the uniaxial tensile strength of concrete, the element is damage. The double lines damage model of residual strength was used in this paper, shown in figure 10. The bending damage variable was defined as:

$$D_t = \begin{cases} 0 & \varepsilon_t < \varepsilon_{t0} \\ 1 - \left(\frac{\lambda - 1}{\eta - 1} + \frac{\lambda - 1}{\eta + 1} \frac{\varepsilon_{t0}}{\varepsilon_t} \right) & \varepsilon_{t0} \leq \varepsilon_t < \varepsilon_{tr} \\ 1 - \frac{\lambda \varepsilon_{t0}}{\varepsilon_t} & \varepsilon_{tr} \leq \varepsilon_t < \varepsilon_{tu} \\ 1 & \varepsilon_{tu} \leq \varepsilon_t \end{cases} \quad (5.2)$$

Here, f_t and f_{tr} are uniaxial tensile strength and ultimate tensile strength, ε_{t0} , ε_{tr} , and ε_{tu} are elastic ultimate tensile strain, strain relative to residual strength and ultimate strain respectively. $\lambda = f_{tr} / f_t$, is residual strength coefficient. $\eta = \varepsilon_{tr} / \varepsilon_{t0}$, is residual strain coefficient. $\xi = \varepsilon_{tu} / \varepsilon_{t0}$, is ultimate strain coefficient. ε_t is principal tensile strain. In this paper, $\lambda = 0.1$, $\eta = 2.0$, $\xi = 0.5$.

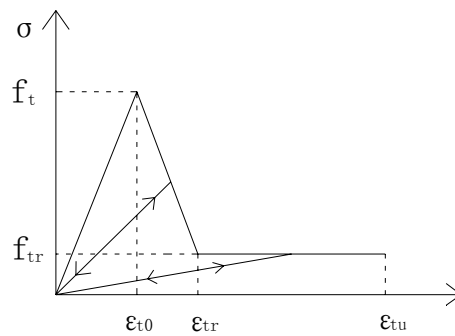


Figure 10 Double lines damage model of residual strength

5.2. Numerical Results Analysis

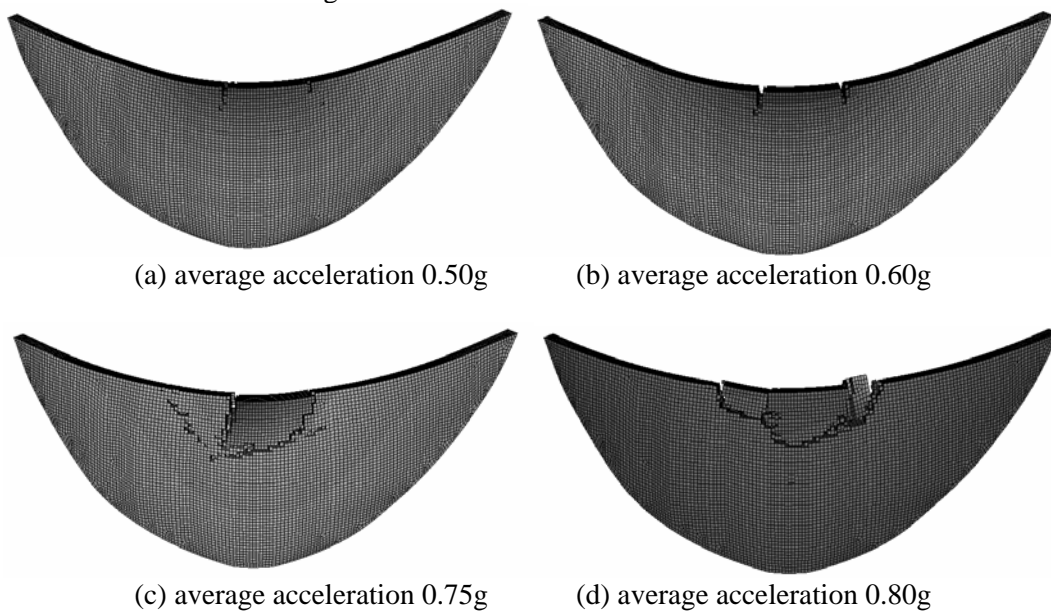
Figure 12 is the final failure mode calculated by numerical analysis. Two cracks appeared when the acceleration reached 0.5g near the upper zone of arch dam, extending down to 1/6 dam height. The cracks were the surface cracks, did not run through the dam. No damage was found in other part. On the downstream face, two cracks appeared at corresponding position when the acceleration reached 0.60 g, the cracks ran through out the dam. The crack extended downward as the load increased. Until the input was 0.75 g, the dam fragment split away. Final failures of model dam calculated by numerical analysis are in agreement with the test results



(a) upstream view

(b) downstream view

Figure 11 Final failures of model dam



(a) average acceleration 0.50g

(b) average acceleration 0.60g

(c) average acceleration 0.75g

(d) average acceleration 0.80g

Figure 12 Final failures of model dam calculated by numerical analysis

6. CONCLUSIONS

The shaking table test and numerical analysis have been performed to investigate the responses and failure process of an arch dam under seismic condition. In model test, arch dam and partial elastic foundation have been simulated. The results show that the weak zone was roughly located in the top of arch crown and one-quarter points of both sides. The failure mode of arch dam is relative to the low order models. The first natural frequency of the model dam was antisymmetric and the second was symmetric, and two frequencies were very close (52 and 54 Hz respectively). The third natural frequency was 71.4 Hz and out of the limit of the shaking table. The finite model analysis showed that the first model participation coefficient was 0.234 times of the second in stream direction. So the dam dynamic responses were the interactive effect of the first and second mode in the vertical and stream direction seismic excitation. Zones near three critical points of the antisymmetric mode, the top of arch crown and one-quarter points of both sides, became the weakness. The use of special concrete is suggested for these zones. The results of the numerical simulations indicate final failures of model dam calculated using the double lines damage model of residual strength are in agreement with the test results.

ACKNOWLEDGEMENTS

The writers are grateful for NSFC (No.90510018 and No.50679006) and NCET (No. 06-0270).

REFERENCES

- J. Zhou, G. Lin, T. Zhu, A. D. Jefferson and F. W. Williams. (2000). Experimental investigation into seismic failure of high arch dams. *Journal of Structural Engineering* **126:8**, 926-935.
- Fenves GL, Mojtahedi S., Reimer RB. (1992). Nonlinear earthquake analysis of arch dam/reservoir. *Proceedings of the 10th WCEE* Madrid.
- Chen Houqun, Li Deyu, Hu Xiao, Hou Shunzai. (1995). Nonlinear model test and computation analysis on dynamic behavior of arch dam with contraction joints. *Earthquake Engineering and Engineering Vibration*
- Chen H, Li D, Hu X, and Hou S. (1996). Model test and computation analysis for dynamic behavior of arch dam with contraction joints. *Proceedings of the 11th WCEE* Mexico. **15:4**, 10-25.
- Haibo Wang, and Deyu Li. (2006). Experimental study of seismic overloading of large arch dam. *Earthquake Engineering and Structural Dynamics* **35:2**, 199-216.
- Haibo Wang, and Deyu Li. (2007). Experimental study of dynamic damage of an arch dam. *Earthquake Engineering and Structural Dynamics* **36:3**, 347-366.
- Lin, G., Zhou, J., and Fen, C. Y. (1993). Dynamic model rupture test and safety evaluation of concrete gravity dams. *Dam Engineering* **3**, 144-173.
- Fan Shuli, Chen Jianyun, Zhou Jing, Zhu Tong, and Jin Qiao. (2007). Experimental research on overfall section dynamic rupture of longkaikou project. *Journal of Hydraulic Engineering* **Sup**, 195-199.